VAN-Mode LCoS Cell Operation with Oblique SiO_2 Alignment

1D director model, 2D pixel fringing-field model and twist analysis

D.F.Hakala

October 31, 2026

Table of Contents

1. Summary 1
2. Programs and files 2
3. The cell 3
4. 1D model: static response 4
5. 1D model: dynamic response 6
6. 2D pixel model: fringing fields 7
7. 2D model with twist: pretilt azimuth and PBS reflectance 9
8. Comparison with published work 11
9. Relevance to neutral-atom arrays 12
10. Limitations 12
References 12

1. Summary

This note documents the Python programs in `C:\LCoS\LCoS_Simulations\VAN_mode_lcos_cell_operation` and their output. They model a reflective liquid-crystal-on-silicon (LCoS) cell in vertically aligned nematic (VAN) mode: a negative-$\Delta\varepsilon$ nematic layer between two obliquely evaporated SiO_2 alignment films, on aluminum pixel mirrors over a silicon backplane. The programs go from a single uniform cell (1D) to a row of 6 μm pixels with fringing fields (2D), and then to the full 3D director with twist so that the pretilt can lean at any angle to the pixel edges. All plots against voltage cover 0–7.5 V.

Main results with the default parameters (material constants close to Merck MLC-6608; 3.1 μm cell; 8° pretilt; 550 nm):

- **Threshold and dark state.** The bend Fréedericksz threshold is 2.19 V. At 0 V the 8° pretilt leaves 0.017 waves of retardation, so the crossed-polarizer dark level is 0.28 % of the peak, a contrast of about 360:1.

- **Amplitude modulation.** The crossed-polarizer reflectance peaks at 3.25 V, where the double-pass retardation is half a wave. Above that the reflectance falls again (0.35 at 7.5 V), so an amplitude-mode drive should run from 0 to about 3.3 V.
- **Phase modulation.** The double-pass retardation reaches 0.80 waves at 7.5 V, against a theoretical maximum of 0.94 waves ($2d\Delta n/\lambda$). This cell cannot give a full 2π of phase at 550 nm.
- **Speed.** The natural relaxation time $\tau_0 = \gamma_1 d^2/(K\pi^2)$ is 10.0 ms. Switching on takes 22 ms at 3 V, 6.4 ms at 5 V and 2.4 ms at 7.5 V (10–90 %); switching off takes 16–17 ms whatever the starting voltage.
- **Fringing fields at a 6 µm pitch** (one pixel driven, neighbors at 0 V, pretilt across the pixel edges). At 3 V the pixel-average phase is only half the 1D value (0.21 against 0.43 waves). No part of the pixel is within 10 % of the intended phase until 3.5 V, and only 50 % of the pitch is at 5 V. A reverse-tilt domain 0.7 µm wide forms at 2.5–3 V and disappears by 5 V. Crosstalk into the neighbors is negligible (≤ 0.0023 waves).
- **Twist when the pretilt leans at 45° to the pixel edges** (the usual operating geometry, PBS axes along the pixel edges). The fringe field twists the director by up to 70° near the pixel edges. The pixel-average reflectance peaks at about 0.51 at 4 V for a 6 µm pitch (0.57 for 8.5 µm), compared with 0.98 for an infinitely large pixel.

2. Programs and files

Program	What it does	Main outputs
`van_lcos_simulation.py`	1D director profile θ(z) across the cell against voltage; static response, tilt map and dynamic step response; Python port of `VAN_Mode_LCoS_Device_Simulation.wl`	`VAN_LCoS_static_response.png`, `VAN_LCoS_tilt_map.png`, `VAN_LCoS_dynamic_response.png`, three CSV files
`van_lcos_pixel2d.py`	2D x–z cross-section through a row of pixels; anisotropic electrostatics coupled to the director; phase across the pixels, effective aperture, reverse tilt, crosstalk	`pixel2d_maps.png`, `pixel2d_sweep.png`, two CSV files
`van_lcos_pixel2d_twist.py`	Same cross-section with a full 3D director (tilt and twist) and an arbitrary pretilt azimuth; Jones-matrix crossed-PBS reflectance	`pixel2d_twist_maps.png`, `pixel2d_twist_sweep.png`, CSV
`van_sio2_cell.py`	Drawing of the cell cross-section with oblique SiO_2 alignment layers (Figure 1)	`setup_C3_VAN_cell_SiO2_alignment.png`

The Mathematica original (`VAN_Mode_LCoS_Device_Simulation.wl`), two reference papers (Nie et al. 2007 on anchoring and response time; Fan-Chiang et al. 2005 on fringing fields in LCoS) and a

shortcut to the pretilt-versus-deposition-angle work are in the same folder. Commands used for this note:

```
python van_lcos_simulation.py --vmin 0 --vmax 7.5 --vstep 0.25 --steps 0:5
0:3 0:7.5 --hysteresis --no-show
python van_lcos_pixel2d.py --voltages 0 1 2 2.5 3 3.5 4 5 6 7 7.5 --map-volts
3 5 --no-show
python van_lcos_pixel2d_twist.py --compare 0 45 90 --voltages 0 2 2.5 3 3.5 4
5 6 7 7.5 --no-show
python van_lcos_pixel2d_twist.py --compare 0 45 90 --pitch-um 8.5 --voltages
0 2 2.5 3 3.5 4 5 6 7 7.5 --outdir tw85 --no-show
python van_sio2_cell.py
```

The 1D run takes about 3 seconds, the 2D pixel run about 4 minutes and each twist comparison 2–3 minutes. In my copy of `van_lcos_simulation.py` the tilt-map axis was also limited to the sweep range so that it stops at 7.5 V (one line; the original pads it by half a step).

3. The cell

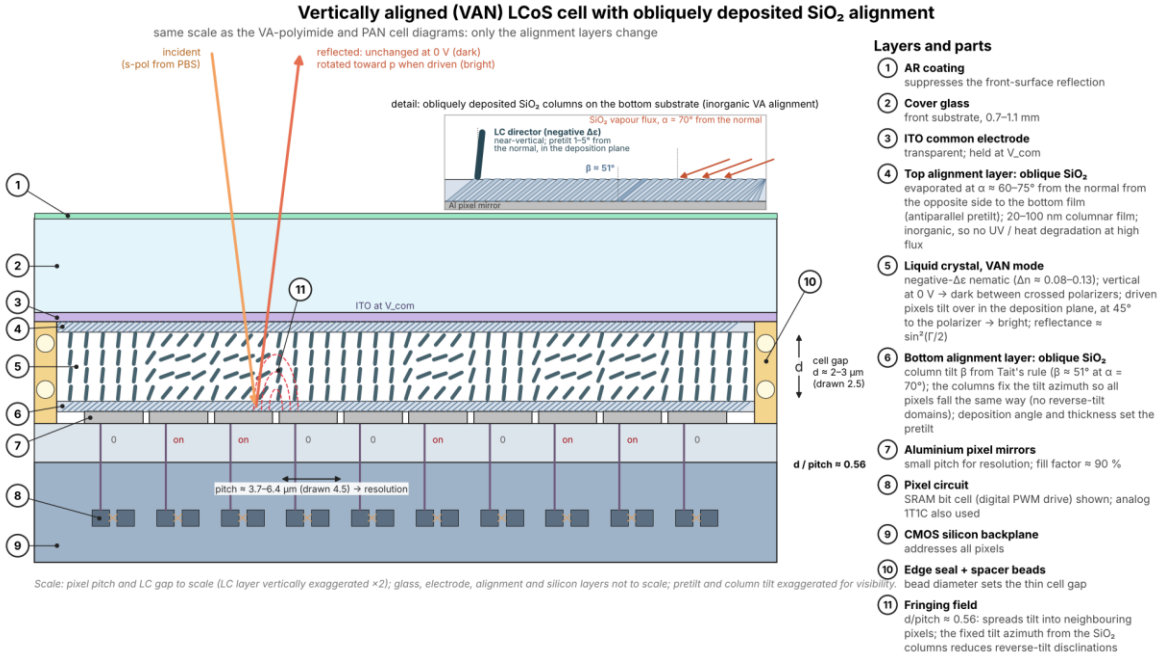


Figure 1. VAN LCoS cell with obliquely deposited SiO_2 alignment layers (van_sio2_cell.py). The inset shows the columnar SiO_2 film; the column tilt follows Tait's rule. Pixel pitch and cell gap are drawn to scale with the LC layer exaggerated two times vertically.

The modeled stack is ITO-coated cover glass, top SiO_2 alignment layer, about 3.1 µm of negative-Δε nematic, bottom SiO_2 alignment layer, and an 800 Å aluminum pixel mirror on the silicon backplane. At 0 V the director stands nearly perpendicular to the substrates, tilted by the pretilt toward the azimuth of the SiO_2 columns, so the cell looks isotropic at normal incidence and is dark between crossed polarizers. A pixel voltage tilts the director over, in the deposition plane, giving birefringence. The SiO_2 column tilt β follows Tait's rule,

$$\beta = \alpha - \arcsin\left(\frac{1-\cos\alpha}{2}\right) \tag{3.1}$$

for deposition angle α from the substrate normal (β ≈ 51° at α = 70°). The drawing uses a 2.5 µm cell, a 4.5 µm pitch and a 1–5° pretilt as typical values; the simulations below use 3.1 µm, 6 µm (and 8.5 µm) and 8°.

Parameter	Value used	Notes
Cell gap d	3.1 µm	
Pretilt (both surfaces)	8° from the normal	fixed input; strong anchoring
Splay, bend constants K_{11}, K_{33}	16.7, 18.1 pN	MLC-6608
Twist constant K_{22}	7.0 pN	twist model only; illustrative
$\varepsilon_\perp$, $\varepsilon_\parallel$ ($\Delta\varepsilon$)	7.6, 3.4 (−4.2)	
Rotational viscosity γ_1	0.186 Pa·s	
n_o, n_e (Δn)	1.500, 1.583 (0.083)	
Wavelength	550 nm	
Pixel pitch, gap	6.0 µm, 0.5 µm (silica fill, ε = 3.9)	2D models

4. 1D model: static response

The director is n = (sin θ, 0, cos θ) with θ(z) the tilt from the cell normal. The Frank elastic energy per unit volume is

$$f_{el} = 1/2\,(K_{11}\sin^2\theta + K_{33}\cos^2\theta)\theta'^2 \tag{4.1}$$

With no free charge, the displacement D is uniform through the cell, and the field follows from the applied voltage V and the local permittivity $\varepsilon_{eff} = \varepsilon_\perp + \Delta\varepsilon\cos^2\theta$:

$$E(z) = \frac{V}{\varepsilon_{eff}(z)\int_0^d \frac{dz'}{\varepsilon_{eff}(z')}} \tag{4.2}$$

The program minimizes the total energy $F = \int f_{el}\,dz - \tfrac{1}{2}CV^2$ (C the cell capacitance per unit area) on a 61-point grid with strong anchoring at the pretilt, using L-BFGS followed by a Newton polish. The threshold of an ideal homeotropic cell is the bend Fréedericksz voltage

$$V_{th} = \pi\sqrt{\frac{K_{33}}{\varepsilon_0(-\Delta\varepsilon)}} \tag{4.3}$$

which is 2.19 V here; the pretilt rounds off the knee. For the optics, each slice contributes the local index difference $n_{eff}(\theta) - n_o$, with

$$n_{eff}(\theta) = \left(\frac{\cos^2\theta}{n_o^2} + \frac{\sin^2\theta}{n_e^2}\right)^{-1/2} \tag{4.4}$$

and the reflective (double-pass) retardation is $\Gamma = (4\pi/\lambda)\int(n_{eff} - n_o)dz$. With the director at 45° to crossed polarizers, the reflectance is

$$R = \sin^2(\Gamma/2) \tag{4.5}$$

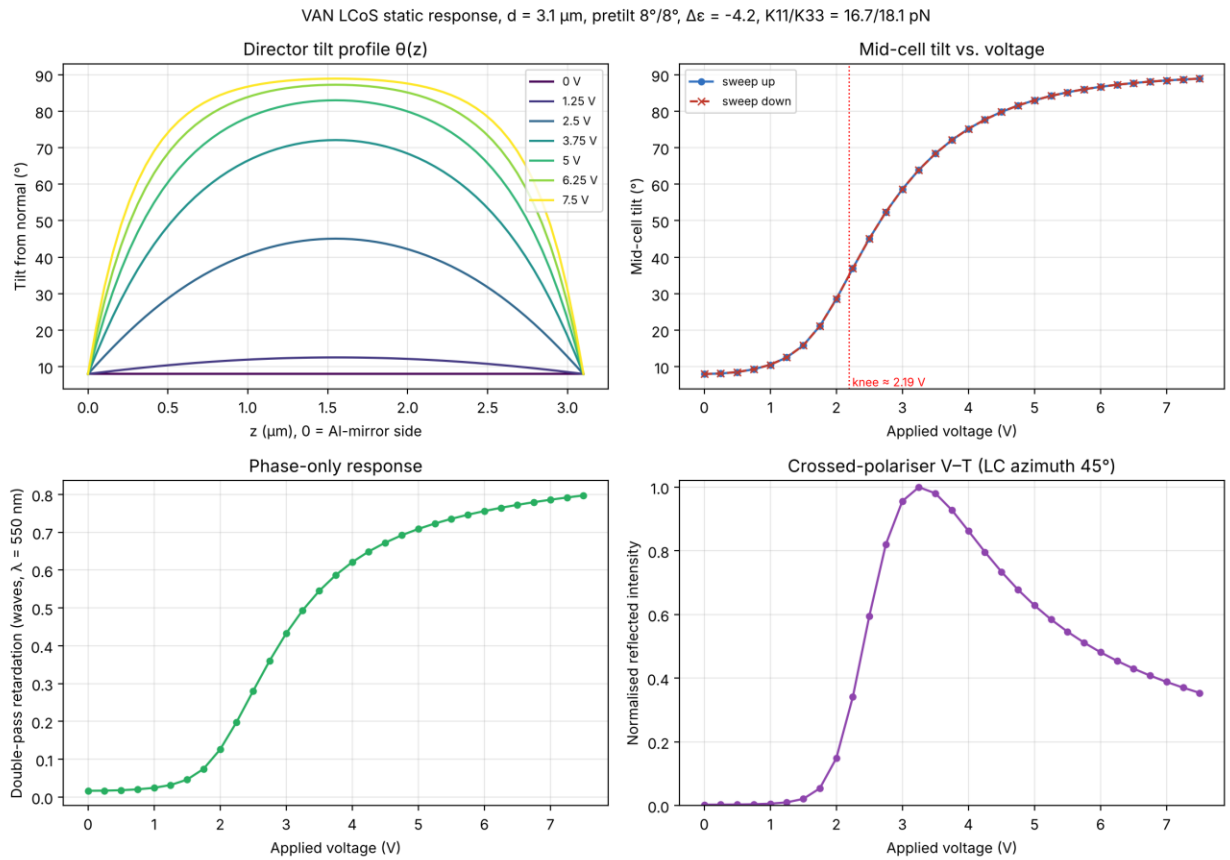


Figure 2. 1D static response, 0–7.5 V: tilt profiles, mid-cell tilt (sweep up and down), double-pass retardation and crossed-polarizer reflectance.

V (V)	Mid-cell tilt (°)	Retardation (waves)	Crossed-pol. R
0	8.0	0.017	0.003
1.0	10.5	0.025	0.006
2.0	28.5	0.126	0.148
2.5	45.1	0.280	0.595
3.0	58.6	0.433	0.956
3.25	63.9	0.494	1.000
4.0	75.2	0.621	0.862
5.0	83.0	0.709	0.628
6.0	86.7	0.756	0.481
7.5	88.9	0.797	0.354

Table 4.1. 1D static response (VAN_LCoS_static_results.csv; 0.25 V steps in the file).

The sweep down retraces the sweep up to within 4×10^{-10} degrees, so the cell has a single stable state at every voltage (no hysteresis). Figure 3 shows the whole tilt field: the director tilts first at mid-cell, and above about 5 V the middle 2 µm is nearly horizontal while thin boundary layers stay anchored at the pretilt.

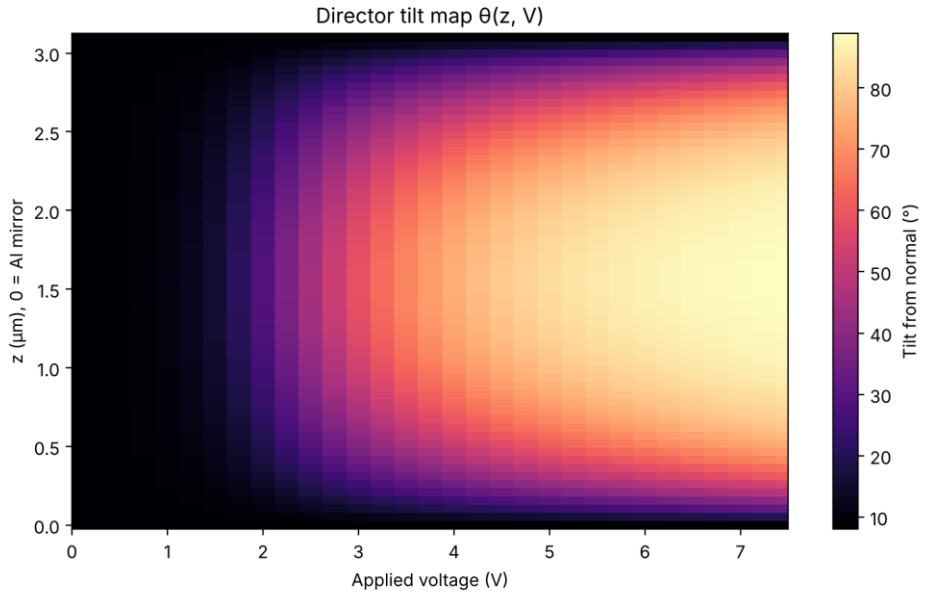


Figure 3. Director tilt θ(z, V) across the cell, 0–7.5 V.

Dark level and pretilt. The residual 0.017 waves at 0 V comes from the 8° pretilt and sets the dark-state reflectance at 0.28 %. Because the residual retardation scales roughly as $\sin^2\theta_p$ and the dark reflectance as its square, reducing the pretilt to 3° would lower the dark level by roughly a factor of 50, at the cost of a sharper threshold and a greater risk of reverse-tilt domains (Section 6).

Usable phase range. The maximum double-pass retardation of a 3.1 µm cell with Δn = 0.083 is $2d\Delta n/\lambda = 0.94$ waves at 550 nm; 0.80 waves is reached at 7.5 V because the boundary layers never tilt fully. For amplitude modulation this is ample (half a wave is needed). For phase-only use, which needs at least one full wave, it is not.

5. 1D model: dynamic response

Without backflow the director relaxes as

$$\gamma_1 \frac{\partial \theta}{\partial t} = g\,\theta'' + 1/2\, g'(\theta)\,\theta'^2 - 1/2\,\varepsilon_0\,\Delta\varepsilon\,\sin 2\theta\,E^2 \qquad (5.1)$$

with $g(\theta) = K_{11}\sin^2\theta + K_{33}\cos^2\theta$. The program integrates the gradient flow of the same discrete energy used for the static states (implicit BDF), so the dynamic end states agree exactly with Section 4. The characteristic time is $\tau_0 = \gamma_1 d^2/(K_{33}\pi^2) = 10.0$ ms.

Step	Rise, 10–90 % (ms)	Fall, 90–10 % (ms)
0 ↔ 3 V	22.3	15.8
0 ↔ 5 V	6.4	16.6

Step	Rise, 10–90 % (ms)	Fall, 90–10 % (ms)
0 ↔ 7.5 V	2.4	17.2

Table 5.1. Switching times of the double-pass retardation.

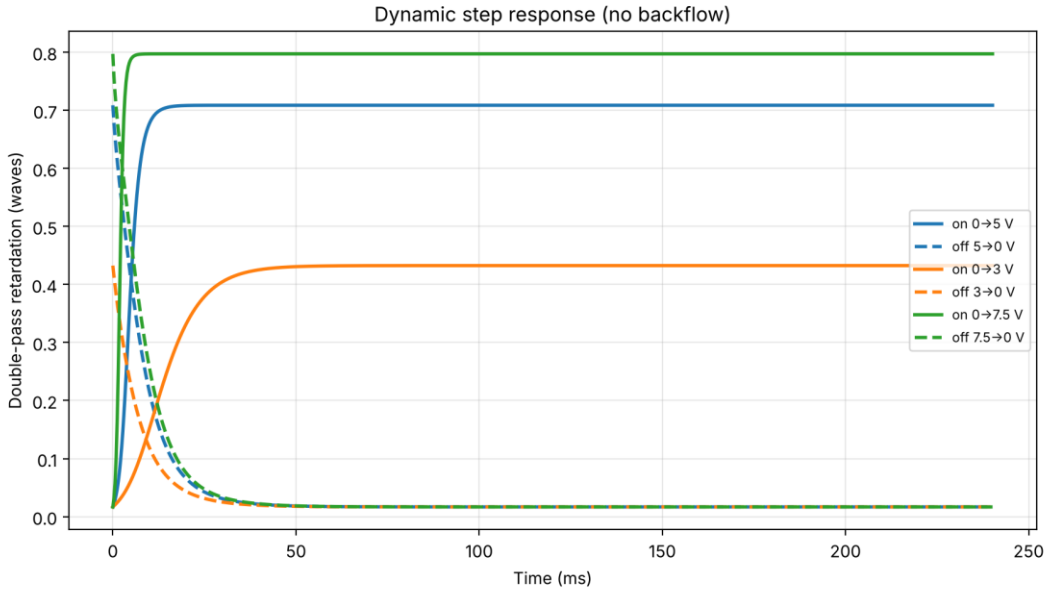


Figure 4. Retardation against time after switching on (solid) and off (dashed) for 0 ↔ 3, 5 and 7.5 V.

Switching on speeds up strongly with voltage because the field torque grows as V^2. Switching off is driven only by elasticity and takes about $1.6\tau_0$ whatever the starting voltage. Since τ_0 scales as d^2, a thinner cell is the main lever for speed: 2.5 µm would cut the fall time by about 35 %. Nie et al. (2007) show that with weak anchoring the scaling drops toward d^1; the SiO_2 anchoring strength is not yet known.

6. 2D pixel model: fringing fields

`van_lcos_pixel2d.py` solves the coupled director and potential in an x–z cross-section through three 6 µm pixels (periodic in x), with 5.5 µm aluminum mirrors, 0.5 µm silica-filled gaps and the ITO at 0 V. The electrostatics use the full anisotropic permittivity,

$$\nabla \cdot (\varepsilon_0\, \boldsymbol{\varepsilon}(\theta)\, \nabla\phi) = 0, \qquad \boldsymbol{\varepsilon} = \varepsilon_\perp \mathbf{I} + \Delta\varepsilon\, \mathbf{n}\mathbf{n}^T \tag{6.1}$$

re-solved for every director state, and the elastic energy is the splay-bend form for an in-plane director,

$$f_{el} = 1/2\, K_{11}(\cos\theta\, \theta_x - \sin\theta\, \theta_z)^2 + 1/2\, K_{33}(\sin\theta\, \theta_x + \cos\theta\, \theta_z)^2 \tag{6.2}$$

discretized with linear finite elements on a 180 × 65-node mesh (23 040 triangles) and minimized with L-BFGS, stepping up in voltage. The center pixel is driven and its neighbors held at 0 V. The pretilt leans in this cross-section, perpendicular to the pixel edges, which is the direction in which fringe fields oppose the pretilt at one edge.

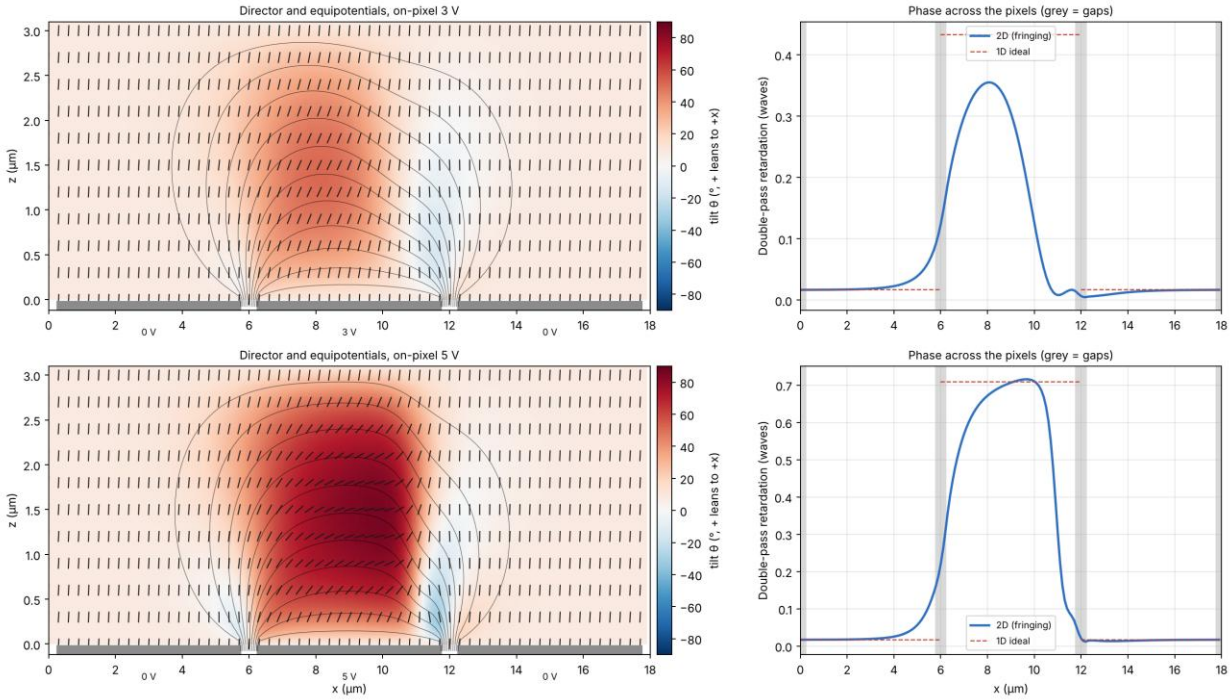


Figure 5. Director, equipotentials and phase across three pixels with the center pixel at 3 V (top) and 5 V (bottom). Red: tilt toward +x; blue: reverse tilt.

V_{on} (V)	Pixel-mean phase (waves)	Center phase (waves)	1D phase (waves)	Aperture (% of pitch)	Reverse tilt (µm)
2.0	0.055	0.059	0.126	0	0
2.5	0.110	0.137	0.280	0	0.70
3.0	0.208	0.305	0.433	0	0.70
3.5	0.320	0.486	0.545	11.7	0.50
4.0	0.419	0.601	0.621	31.7	0.20
5.0	0.560	0.707	0.709	50.0	0
6.0	0.649	0.755	0.756	58.3	0
7.5	0.725	0.797	0.797	66.7	0

Table 6.1. 2D fringing-field results for a single driven 6 µm pixel (pixel2d_sweep.csv). "Aperture" is the fraction of the pitch within 10 % of the 1D phase.

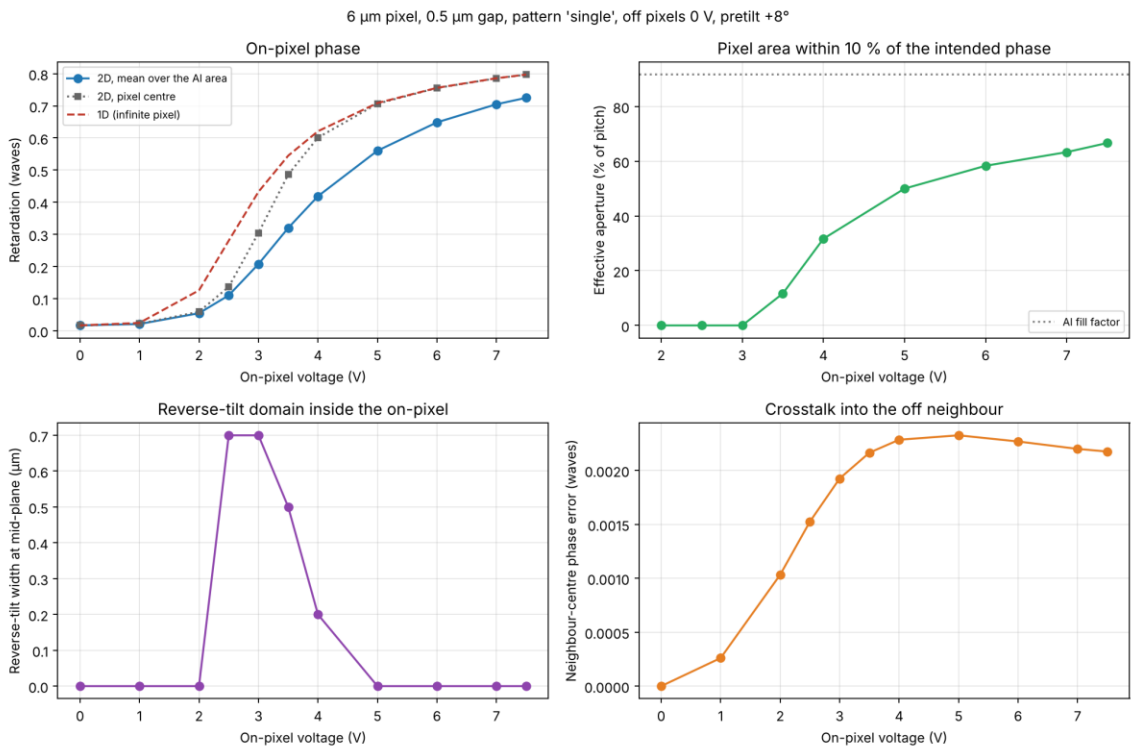


Figure 6. 2D sweep, 0–7.5 V: on-pixel phase against the 1D value, effective aperture, reverse-tilt width and crosstalk.

Three effects stand out:

1. **The pixel responds late and only in part.** With d/pitch ≈ 0.52, the fringe field near the gaps is weaker and tilted, so the pixel-average phase lags the 1D value by a factor of two at 3 V. The center catches up above about 5 V, but even at 7.5 V only two thirds of the pitch is within 10 % of the target phase, compared with a 92 % mirror fill factor.
2. **Reverse tilt.** Near the right-hand edge (where the field line slope opposes the pretilt), the director tips the wrong way over a 0.7 µm band at 2.5–3 V (blue in Figure 5). It shrinks as the voltage rises and is gone at 5 V. Its boundary would appear as a disclination line in a real cell.
3. **Negligible crosstalk.** The phase at the centers of the off neighbors changes by at most 0.0023 waves, because the 0 V neighbors are held vertical by their own field-free state.

7. 2D model with twist: pretilt azimuth and PBS reflectance

`van_lcos_pixel2d_twist.py` uses the same geometry with the director free in three dimensions,

$$\mathbf{n} = (\sin\theta\cos\psi,\ \sin\theta\sin\psi,\ \cos\theta) \tag{7.1}$$

where ψ is the azimuth from x (x perpendicular to the pixel edges) and ψ_0 the pretilt azimuth set by the SiO_2 deposition plane. The elastic energy now includes twist,

$$f_{el} = 1/2\,K_{11}(\nabla\cdot\mathbf{n})^2 + 1/2\,K_{22}(\mathbf{n}\cdot\nabla\times\mathbf{n})^2 + 1/2\,K_{33}|\mathbf{n}\times\nabla\times\mathbf{n}|^2 \tag{7.2}$$

The optics are computed per x column with Jones matrices: each slice is a linear retarder along the projected director, the light passes down and back up, and the output is the crossed-PBS reflectance

with the PBS axes along the pixel edges. For a uniform cell with ψ = 45° this reduces exactly to Equation 4.5, and energy is conserved to about 10^{-14} in every column.

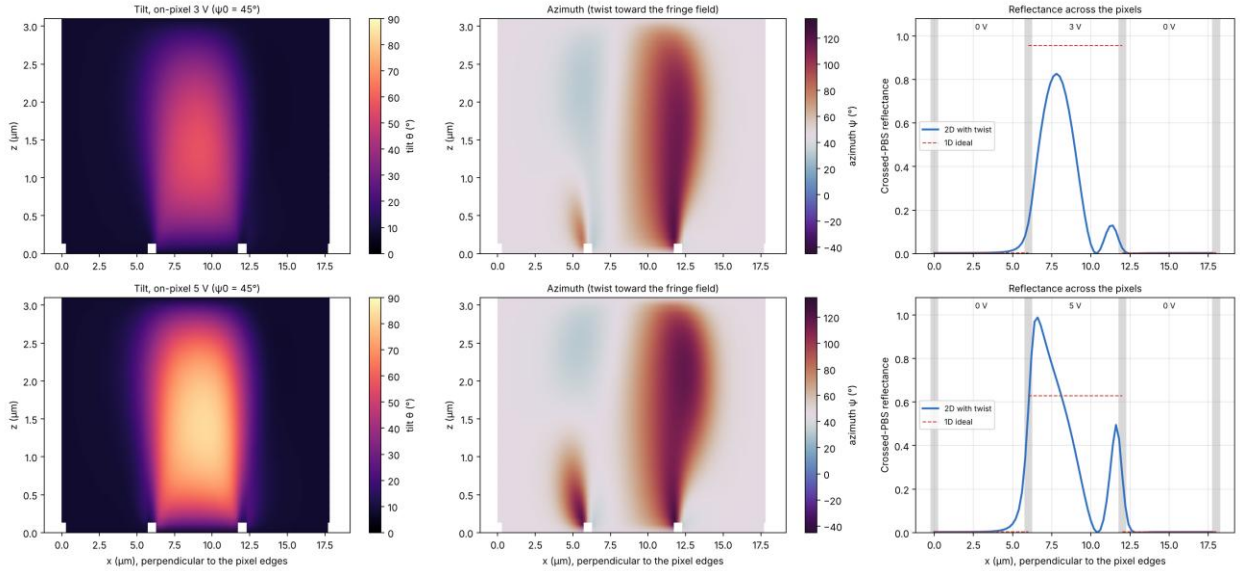


Figure 7. Tilt, azimuth and crossed-PBS reflectance across three 6 µm pixels for ψ_0 = 45°, center pixel at 3 V (top) and 5 V (bottom).

V_{on} (V)	R, 6 µm pitch	R, 8.5 µm pitch	R, 1D ideal	Max twist, 6 µm (°)
2.0	0.052	0.070	0.148	59
2.5	0.203	0.267	0.595	67
3.0	0.396	0.485	0.956	69
3.5	0.497	0.572	0.980	70
4.0	0.514	0.568	0.863	69
5.0	0.456	0.485	0.629	67
6.0	0.382	0.402	0.482	65
7.5	0.300	0.313	0.355	62

Table 7.1. On-mirror average crossed-PBS reflectance for ψ_0 = 45° (pixel2d_twist_sweep.csv for each pitch).

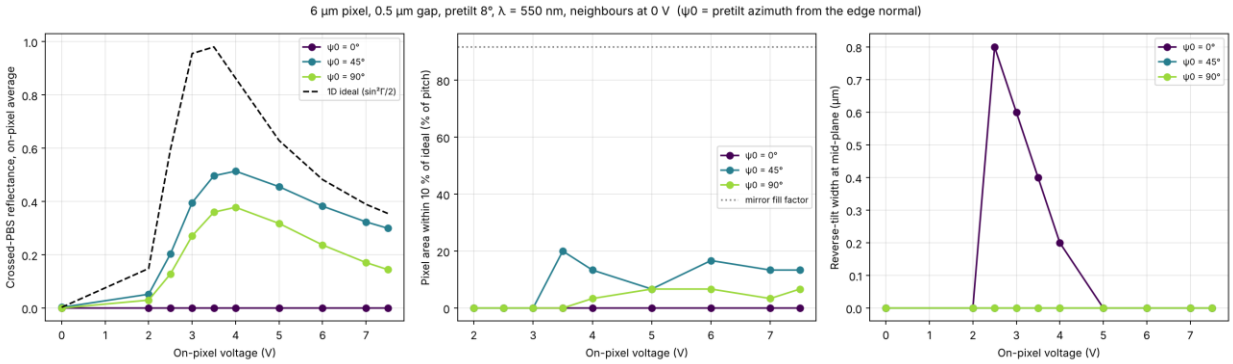


Figure 8. Twist model sweep for a 6 µm pitch, 0–7.5 V, for pretilt azimuths of 0°, 45° and 90°: pixel-average reflectance, effective aperture and reverse-tilt width.

The lateral component of the fringe field pulls the director's azimuth toward x, so near both pixel edges the director twists by up to about 70° from the 45° pretilt azimuth (Figure 7, center). Where the azimuth passes through 0° or 90° the director lies along a PBS axis and the column goes dark, which carves a dark band about 1 µm wide inside the right-hand side of the driven pixel. As a result, the pixel-average reflectance tops out at 0.51 for a 6 µm pitch and 0.57 for 8.5 µm, about half the 1D value, and the peak moves from 3.25 V to about 4 V. Pixels in a uniformly driven area would not suffer this, because the lateral field cancels; the loss applies to edges, isolated pixels and fine image detail.

Reverse tilt appears only for $\psi_0 = 0°$ (0.8 µm at 2.5 V for 6 µm, 1.0 µm for 8.5 µm), confirming that leaning the pretilt at 45° to the edges suppresses reverse-tilt domains. Note, however, that the script keeps the PBS axes along the pixel edges for every ψ_0. With $\psi_0 = 0°$ or 90° the director then lies along a PBS axis and gives almost no reflectance by construction, so those two curves show edge effects rather than a fair alternative operating point. A fair comparison of pretilt azimuth would rotate the PBS with ψ_0 so that it always sits at 45° to the director.

8. Comparison with published work

Fan-Chiang, Wu and Chen (2005) simulated six LC modes in high-resolution LCoS with a beam-propagation method and found that the VA mode has the highest contrast but the most severe fringing-field effects, with reduced brightness, poor edge sharpness and slow transitions at small pixels. The 2D results here reproduce that picture: at d/pitch ≈ 0.5 the effective aperture is small near threshold and the twisted edge regions halve the pixel-average reflectance. Their remedy, illumination with circularly polarized light, makes the reflectance independent of the director azimuth and so removes the twist-induced dark band; the Jones-matrix part of `van_lcos_pixel2d_twist.py` could test this by replacing the linear PBS input with circular polarization.

Nie et al. (2007) showed that the LC decay time scales as d^2 for strong anchoring and approaches d^1 for weak anchoring. All models here assume strong anchoring, so the 16–17 ms fall times are the strong-anchoring limit for this material and gap.

9. Relevance to neutral-atom arrays

The same reflective LCoS technology, run as a phase-only SLM, forms the static tweezer arrays in neutral-atom machines (Hamamatsu X13138-series panels in the Harvard/QuEra systems). Three results bear directly on that use:

1. **Phase range.** A tweezer hologram needs at least one full wave (2π) of double-pass phase at the trap wavelength. This cell gives 0.80 waves at 550 nm; at 852 nm, with slightly lower Δn and 1.55 times the wavelength, it would give only about 0.5 waves. A phase-only SLM at 852 nm needs $d \geq \lambda/(2\Delta n_{eff}) \approx 5$–$6$ μm with $\Delta n \approx 0.08$, or a higher-birefringence LC.
2. **Polarization.** Phase-only operation requires input polarization along the director's tilt plane, i.e. along the SiO_2 deposition azimuth, with no $\lambda/4$ in the path. The twist found near pixel edges (Section 7) mixes polarizations there, so steep phase gradients in a hologram will scatter light into the orthogonal polarization and lower diffraction efficiency.
3. **Fringing and phase fidelity.** At a 6 μm pitch, a pixel only reaches its target phase over half to two thirds of its width. Holograms with rapid pixel-to-pixel phase changes (large deflection angles, many closely spaced traps) therefore lose efficiency to fringing, which is why tweezer SLMs use 12.5 μm or larger pixels and relatively thick cells.

10. Limitations

- Material constants are close to MLC-6608 but K_{22} and the dielectric values should be checked against the datasheet; times scale as γ_1/K.
- Strong anchoring at a fixed 8° pretilt on both surfaces, including over the pixel gaps; the SiO_2 anchoring energy and the actual pretilt from the deposition angle are not yet measured.
- No backflow, ions, flexoelectricity or series voltage drop in the SiO_2 and ITO layers; ideal RMS drive.
- 2D models assume no variation along the pixel edges, so pixel corners need a full 3D model.
- Optics are per-column (local index or Jones), at normal incidence, with no diffraction inside the 3 μm layer; at a 6 μm pitch a beam-propagation or FDTD step would change the edge profiles.
- In the twist model, the PBS axes are fixed along the pixel edges for all pretilt azimuths (Section 7).

References

1. K.-H. Fan-Chiang, S.-T. Wu and S.-H. Chen, "Fringing-field effects on high-resolution liquid crystal microdisplays," *J. Display Technol.* **1**, 304 (2005) (copy in this folder).
2. X. Nie, R. Lu, H. Xianyu, T. X. Wu and S.-T. Wu, "Anchoring energy and cell gap effects on liquid crystal response time," *J. Appl. Phys.* **101**, 103110 (2007) (copy in this folder).
3. P. G. de Gennes and J. Prost, *The Physics of Liquid Crystals*, 2nd ed. (Oxford University Press, 1993).
4. R. N. Tait, T. Smy and M. J. Brett, "Modelling and characterization of columnar growth in evaporated films," *Thin Solid Films* **226**, 196 (1993) (column-tilt rule, Equation 3.1).

5. Merck KGaA, MLC-6608 liquid-crystal data (source of the material constants used).
6. `VAN_Mode_LCoS_Device_Simulation.wl`, LCoS Simulations folder (original Mathematica model).